Robust Halftoning with Green-Noise

Daniel L. Lau, Gonzalo R. Arce and Neal C. Gallagher
Department of Electrical and Computer Engineering
University of Delaware
Newark, DE 19716, USA
lau@ee.udel.edu, arce@ee.udel.edu, gallaghe@ee.udel.edu

Abstract

Green-noise halftoning is a stochastic halftoning technique where the minority pixels of a binary dither pattern form homogeneously distributed pixel clusters. While clustering pixels increases its visibility, green-noise reduces the perimeter-to-area ratio of printed dots, thereby reducing the effects of printer distortions such as dot-gain and dot-loss. Using a stochastic dot model, several techniques are introduced for improving the spatial resolution of error diffusion with output-dependent feedback, a commonly used technique for generating green-noise halftone patterns.

1. Introduction

Previously, research in digital halftoning has focused on the visual appearance of binary dither patterns assuming an ideal printer model where the output patterns are composed of perfectly square black and white dots. While results have shown that blue-noise halftoning is the optimal technique for minimizing halftone visibility [1] and maximizing the apparent spatial resolution [2], the vast majority of printing processes still rely on CDOD due to the reliability of many devices to reproduce isolated dots. Blue-noise, "is generally still considered to be an option only for very high-quality printing situations [3]." The reason for using CDOD is that resulting patterns, composed of clustered dots, are resilient to the distortions of the printing process. A quality referred to as *halftone robustness*. Recent work in halftoning has focused on this problem of printer distortions and the need for robust halftoning.

In printers, dot-gain is the increase in size of a printed dot from its intended size. In the case of mechanical dot-gain, this increase in size is created by the physical spreading of ink as it is applied to the paper during the printing process. Optical dot-gain is the apparent growth of a printed dot created by the interactions of incident light and paper [4]. In either case, dot gain is not, in general, considered a "bad" thing, and its occurrence, either high or low, does not limit the choice in halftoning techniques for a given printing process. What does limit the choice, in halftoning, is the repeatability of dot-gain.

If a printer consistently reproduces dots with little variation in dot gain, accurate tone reproduction can be achieved through tone correction–a process where all pixels of the input image with gray level g are replaced by pixels with gray level g' such that the halftoned image has apparent gray levels as close as possible to those of the original image. The underlying assumption is that when trying to reproduce gray level g', the printer will consistently produce the apparent gray level g. The problem for tone correction occurs when the printer does not produce dot gain consistently. In these instances, it may be more desirable to use a halftoning scheme which resists dot gain by forming clusters, reducing the perimeter-to-area ratio of printed dots [5] and making processes such as tone correction more applicable.

Dot-loss, the inability of a printing device to print an isolated black dot, is particularly common in laser printers when toner is low as demonstrated in Fig. 1. Here, the characteristics of the printed dot change dramatically near the sides of the page, resulting in horrendous tonal distortion when dots are isolated (Fig. 1 (left)). Clustered-dot ordered dither (CDOD) (Fig. 1 (right)), on the other hand, shows little distortion due to the robustness achieved by clustering minority pixels. The drawback of CDOD is that, in some instances, an unnecessary amount of spatial resolution may be sacrificed for pattern robustness. While reducing the size of clusters will increase the apparent spatial resolution, any increase will fall far short of the spatial resolution achieved through adaptive halftoning techniques such as error diffusion.

An alternative to CDOD which intentionally clusters minority pixels is error-diffusion with output-dependent feedback (ODF) [6]. Introduced to address the problems of printing in the presence of distortion, ODF is one of many techniques which generates *green-noise*–stochastic dither patterns composed of homogeneously distributed minority pixel clusters [5]. Being a stochastic arrangement of dots, green-noise avoids the problems of periodic structure and moiré, and as an adaptive technique, achieves a spatial resolution closer to the printing resolution of the device.

ODF's greatest advantage over CDOD, though, is its tunable cluster size, allowing ODF to produce halftone pat-

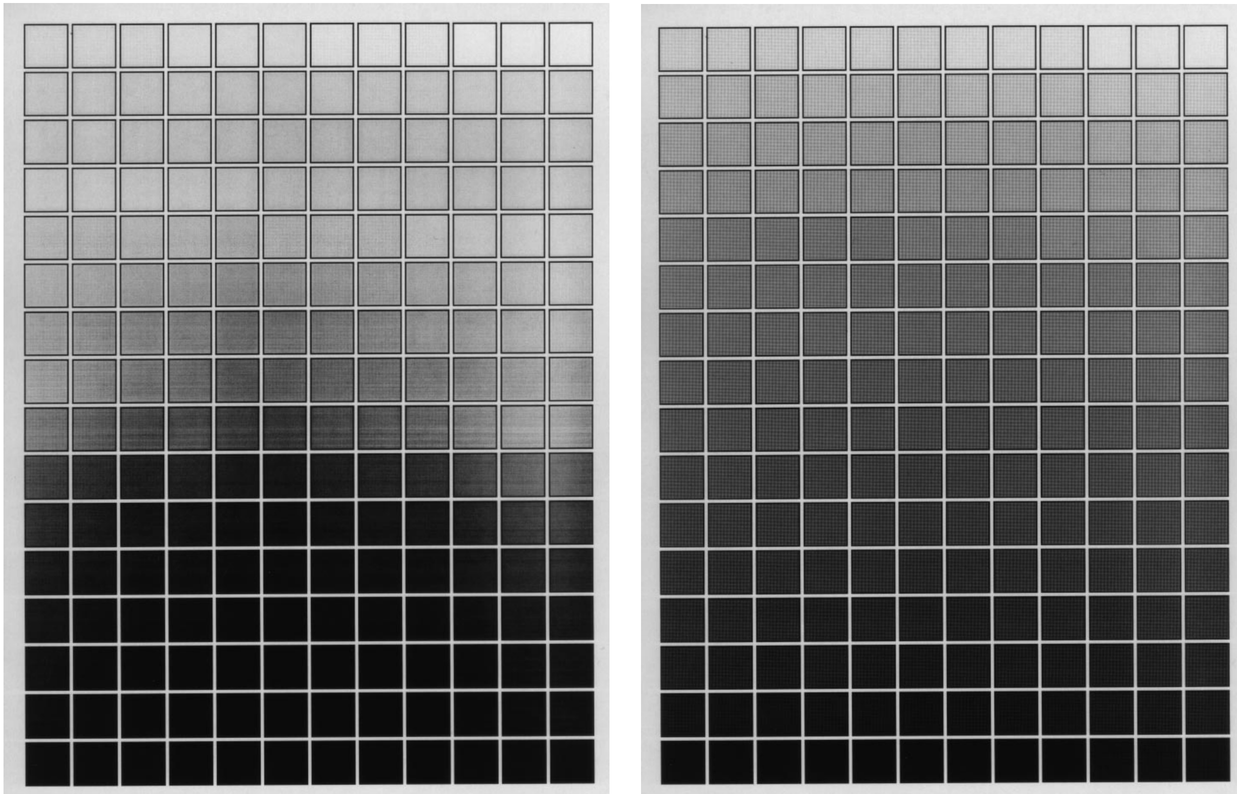

Figure 1: *Gray-scale ramps printed on an Apple LaserWriter Pro 630 using (left) Bayer's dither, illustrating dot-loss, and (right) CDOD with* 8×8 *cells.*

terns composed of large clusters in printers with large variation from printed dot-to-printed dot and small clusters in printers with small variation. Printers, which before were restricted to either AM or FM techniques, can now print AM-FM hybrid patterns which are tuned to offer the highest possible spatial resolution under the constraints of the printer's ability to print individual pixels, and in this paper, using a stochastic dot model, we show how green-noise can be tuned to offer the highest spatial resolution while under the constraints of the printed dot.

2. Stochastic Dot Model

Electro-photographic or laser printers typically use CDOD as these printers are very unreliable at printing individual dots. In laser printers, a laser beam scans across the surface of a photo-conductive drum, leaving the drum positively charged in areas where black dots are to be printed [7]. Toner particles, which are negatively charged, are then attracted to these positions on the drum, forming an image which is then electro-statically transfered to the paper. Through heat and pressure, the toner is then fused to the paper's surface.

In this paper, the probability of a toner particle, at point y given the set of printed dots $\{x_i : i = 1, 2, \ldots, N\}$, is modeled as a function of the total amount of light energy collected, from a laser, by the point on the photo-conductive drum corresponding to y. Assuming a Gaussian beam, this total amount of light, L_y, is defined as:

$$L_y = \sum_{i=1}^{N} \exp^{-\alpha|y-x_i|^2/d^2}, \qquad (1)$$

the superposition of beams corresponding to each printed dot x_i. The parameter d is the minimum distance between samples on the printed page, and α is related to the beam width of the laser. Given L_y, the probability of toner at y is then defined as:

$$P(y; \{x_i : i = 1, 2, \ldots, N\}) = F\left(L_y\right), \qquad (2)$$

where the transfer function $F(\cdot)$ determines how the total amount of light energy collected maps to a probability of a toner particle occurring.

The exact form of $F(\cdot)$ is a function of the printing device which, in order to specify, may require close examination of the physics involved in the process, but for the simplest form of $F(\cdot)$, we propose a function of the two parameters T_1 and T_2 such that:

$$F(L_y) = \begin{cases} 0, & \text{for } L_y < T_1 \\ \frac{(L_y - T_1)}{T_2 - T_1}, & \text{for } T_1 \leq L_y < T_2 \\ 1, & \text{for } T_2 \leq L_y \end{cases} . \quad (3)$$

This form of $F(L_y)$ describes a printer for which an absorbed light intensity less than T_1 will attract no toner to point y while an absorbed intensity greater than T_2 will guarantee toner.

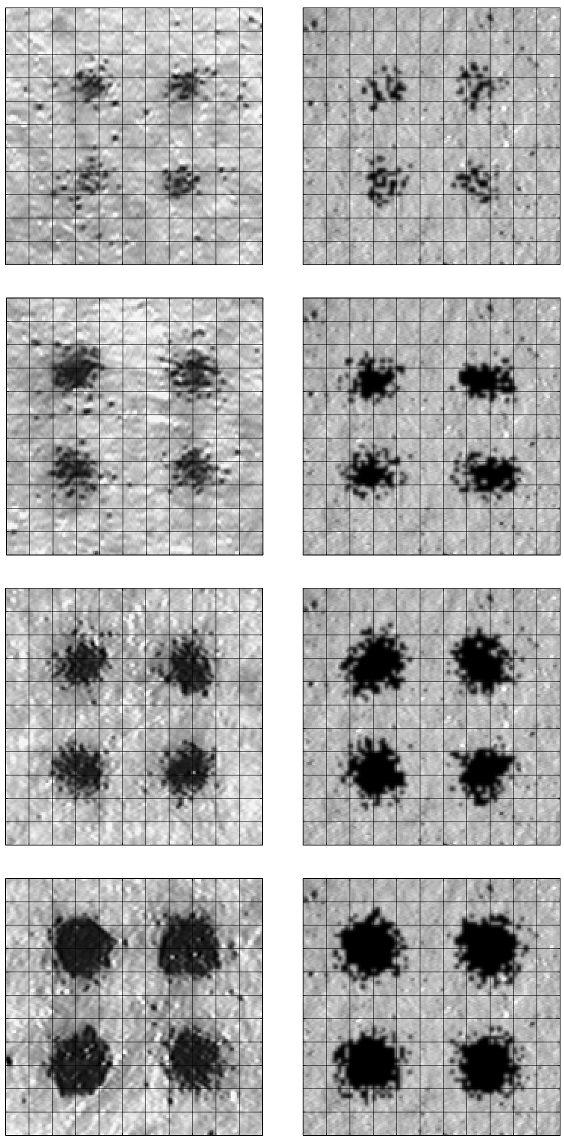

Figure 2: *Dot clusters composed of one, two, three or four black pixels for (a) an Apple LaserWriter Pro 630 printer and (b) a stochastic dot model.*

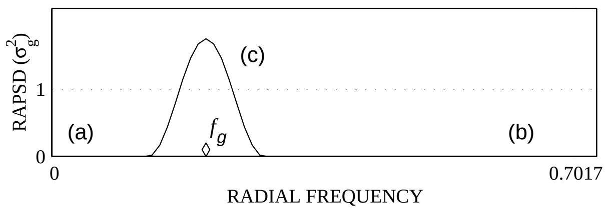

Figure 3: *The radially averaged power spectrum density for the ideal green-noise halftone pattern.*

Fig. 2 illustrates this new model using eqn. (3) with the parameters $\{\alpha, T_1, T_2\} = \{1.11, 0.23, 1.46\}$. An advantage to this newest model is that by employing the superposition of beams, the probability of toner occurring for a particular dot is directly affected by the concentration of dots in the surrounding area, as demonstrated in Fig. 2(bottom) where the modeled output forms a dense macro-dot when composed of four pixels.

3. Green-Noise

Halftoning techniques which create stochastic patternings of clustered dots fall into the general category of green-noise halftoning. Their name, "green-noise", derives from the patterns' mid-frequency only spectral content. This spectral content is best illustrated using Ulichney's *radially averaged power spectrum density* [8] measure where the ideal green-noise pattern has a power spectrum as shown in Fig. 3. The parameter f_g, indicated by a small diamond placed along the horizontal axis, is the *principle frequency* of green-noise and is the inverse of the average distance between nearest clusters. As Lau *et al.* [5] describe, given a green-noise binary dither pattern representing gray level g with an average of M pixels per cluster, the largest spectral components will be found at or near f_g such that:

$$f_g = \begin{cases} \sqrt{(g)/M}/d & , \text{ for } 0 < g \leq 1/2 \\ \sqrt{(1-g)/M}/d & , \text{ for } 1/2 < g \leq 1 \end{cases} \quad (4)$$

where d is, again, the minimum distance between addressable samples on the display.

Fig. 4 shows the impact of green-noise with respect to tone reproduction versus clustered-dot ordered dither and blue-noise halftoning.

3.1. Error Diffusion with Output-Dependent Feedback

Introduced by Levien [6], error diffusion with output dependent feedback is shown in Fig. 5 where the binary output pixel $y[n]$ is defined according to the thresholding function $T(\cdot)$ as:

$$y[n] = T(x[n] + x^e[n] + x^h[n]) \quad (5)$$

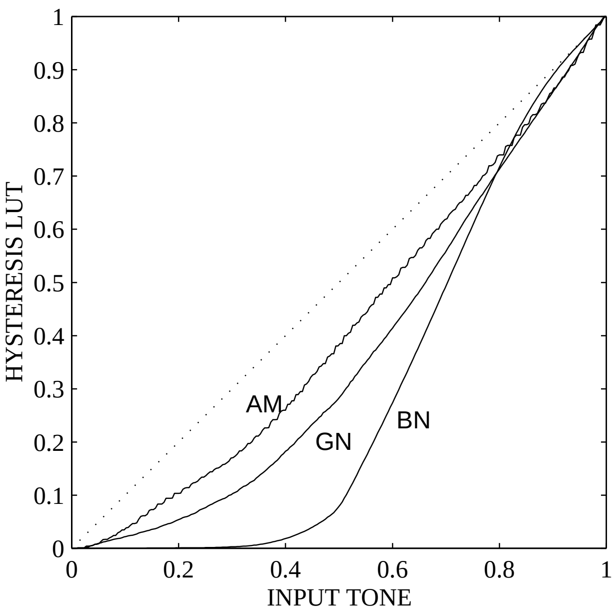

Figure 4: *Modeled tone reproduction curve using clustered-dot ordered dither (8×8 cells), blue-noise, and green-noise halftoning.*

$$= \begin{cases} 1 \quad , & (x[n] + x^e[n] + x^h[n]) \geq 0 \\ 0 \quad , & \text{else} \end{cases} \quad . \quad (6)$$

The error term, $x^e[n]$, is the diffused quantization error accumulated during previous iterations as:

$$x^e[n] \quad = \quad \sum_{i=1}^{M} b_i \cdot y^e[n-i] \qquad (7)$$

where $y^e[n] = y[n] - (x[n] + x^e[n])$ and $\sum_{i=1}^{M} b_i = 1$, and the term, $x^h[n]$, is the hysteresis or feedback term defined as:

$$x^h[n] \quad = \quad h \sum_{i=1}^{N} a_i \cdot y[n-i] \qquad (8)$$

where $\sum_{i=0}^{N} a_i = 1$ and h is an arbitrary constant. Referred to as the *hysteresis constant*, this parameter h acts as a tuning parameter with larger h leading to coarser output textures [6], as h increases ($h > 0$) or decreases ($h < 0$) the likelihood of a minority pixel occurring if the previous outputs were also minority pixels. Fig. 7, using the arrangement of 2 hysteresis and 2 error diffusion coefficients shown in Fig. 6, shows the impact of increasing h where small h (near 0) leads to small clusters and large h (near 2.5) leads to large clusters.

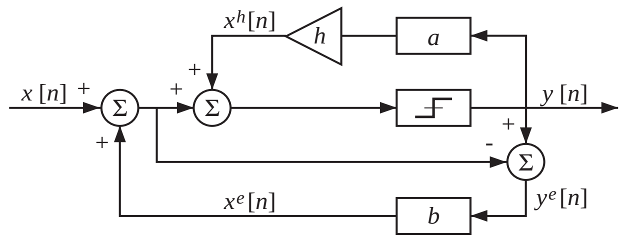

Figure 5: *The error diffusion with output-dependent feedback algorithm as introduced by Levien [6].*

3.2. Tone-Dependent Hysteresis

Optimizing ODF for a given printing process is achieved by specifying the parameter h according to the desired robustness, but as a constant, ODF may, like AM halftoning, sacrifice spatial resolution at certain gray-levels for pattern robustness at other levels. It may, therefore, by advantageous to employ an adaptive hysteresis parameter which varies according to the input gray-level. One such arrangement would be, for each gray-level, to select the minimum h such that the output tone is within a pre-specified tolerance of the input.

Shown in Fig. 8 (left) is the optimal h for each gray-level where h is chosen to maximize the spatial resolution while maintaining an output tone within 50% of the input. Fig. 8 (right) shows the resulting input versus output tone reproduction curve where the tone constraint is plotted as a dotted line. The images of Fig. 9 show the resulting ideal and modeled outputs using tone-dependent hysteresis. Radial symmetry is achieved in these images by allowing the feedback coefficients, a_1 and a_2, to vary with h.

3.3. Frequency-Dependent Hysteresis

Further improvements in spatial resolution may be gained by varying h according to the frequency content of the input image. In this scheme, the resulting halftoned image will be composed of large clusters in DC regions, where distortions are most noticeable to the human eye, and small clusters near edges where distortions are least noticeable and spatial details require small clusters in order to be preserved.

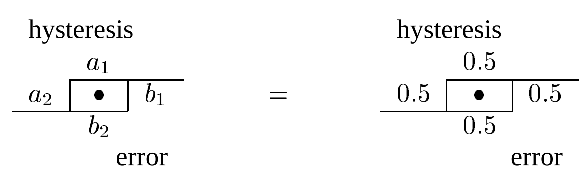

Figure 6: *An arrangement of two hysteresis and two error diffusion coefficients and their corresponding default values.*

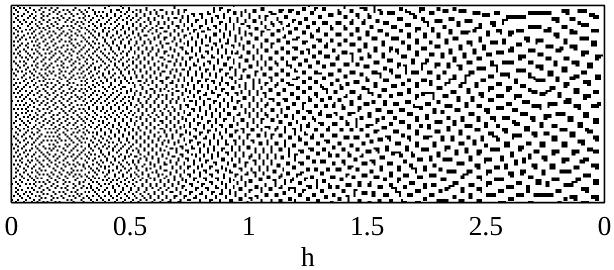

Figure 7: *Halftoned image ($g = 0.75$) showing the effects of increasing h.*

Fig. 10 (top) shows the resulting hysteresis parameter (white=3.0 and black=0.0) used at each pixel to create the ideal printer output image of Fig. 10 (middle) and the modeled printer output image of Fig. 10 (bottom). The improvement in resolution made by using frequency-dependent hysteresis can best be seen in areas of text and around the eyes.

4. Conclusions

Digital halftoning is a technique used by binary display devices to create the illusion of continuous tone. While blue-noise is the optimal technique for achieving high spatial resolution, this paper has shown that due to the unreliability of some printers to print isolated pixels, blue-noise is not always appropriate for halftoning. Instead, these printers need halftoning techniques which intentionally cluster pixels of like color. This clustering makes resulting patterns more resistant to the effects of both dot-gain and dot-loss. By varying a hysteresis parameter, ODF is able to create patterns with adjustable coarseness. ODF can, therefore, be optimized for a specific printing device with the resulting spatial resolution maximized according to the constraints of the printed dot. In this paper, we have shown that an adaptive hysteresis parameter can be employed to either maximize the spatial resolution at each gray-level or maximize the spatial resolution near edges.

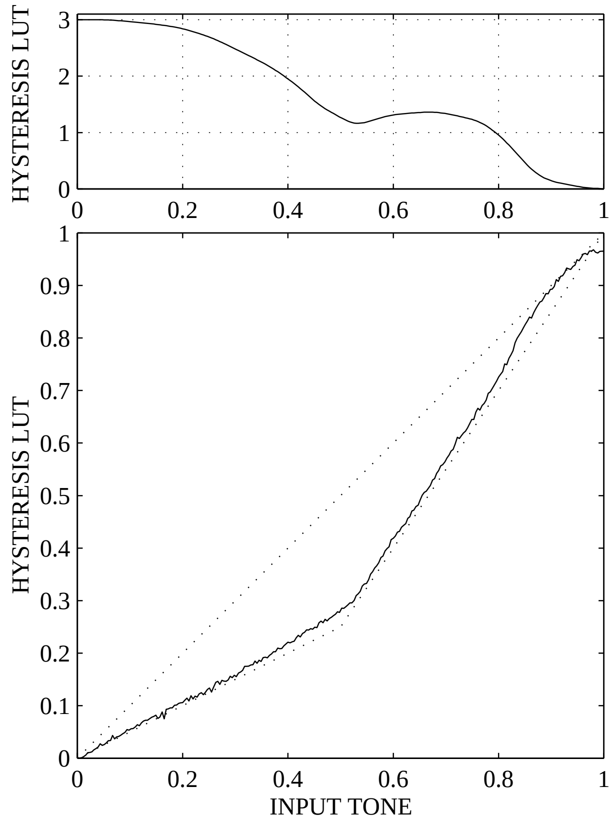

Figure 8: *Look-up table values and tone reproduction curve for tone-dependent hysteresis.*

References

[1] J. Sullivan, L. Ray, and R. Miller, "Design of minimum visual modulation halftone patterns," *IEEE Transactions Syst. Man Cybernet*, vol. 21, no. 1, 1991.

[2] M. Rodriguez, "Graphic arts perspective on digital halftoning," *Proceedings of SPIE, Human Vision, Vision Processing and Digital Display V*, vol. 2179, pp. 144–149, Feb. 1994.

[3] D. Blatner and S. Roth, *Real World Scanning and Halftones*. Addison-Wesley Publishing Company, Berkeley, California, USA, 1993.

[4] B. Kruse and M. Wedin, "A new approach to dot gain modeling," *TAGA Proceedings*, vol. 1, pp. 329–338, 1995.

[5] D. L. Lau, G. R. Arce, and N. C. Gallagher, "Green-noise digital halftoning," *Proceedings of the IEEE*, vol. 86, pp. 2424–2444, Dec. 1998.

[6] R. Levien, "Output dependant feedback in error diffusion halftoning," in *IS&T's Eighth International Congress on Advances in Non-Impact Printing Technologies*, pp. 280–282, Oct. 1992.

[7] I. L. Weiselman and E. Tomash, "Marks on paper: Part 2. a historical survey of computer output printing," *Annals of the History of Computing*, vol. 13, no. 2, pp. 203–222, 1991.

[8] R. A. Ulichney, "Dithering with blue noise," *Proceedings of the IEEE*, vol. 76, Jan. 1988.

Figure 9: *The modeled output of the image Adrian after halftoning with (top) blue-noise, (middle) green-noise with $h = 2.0$, and (bottom) green-noise with tone-dependent h.*

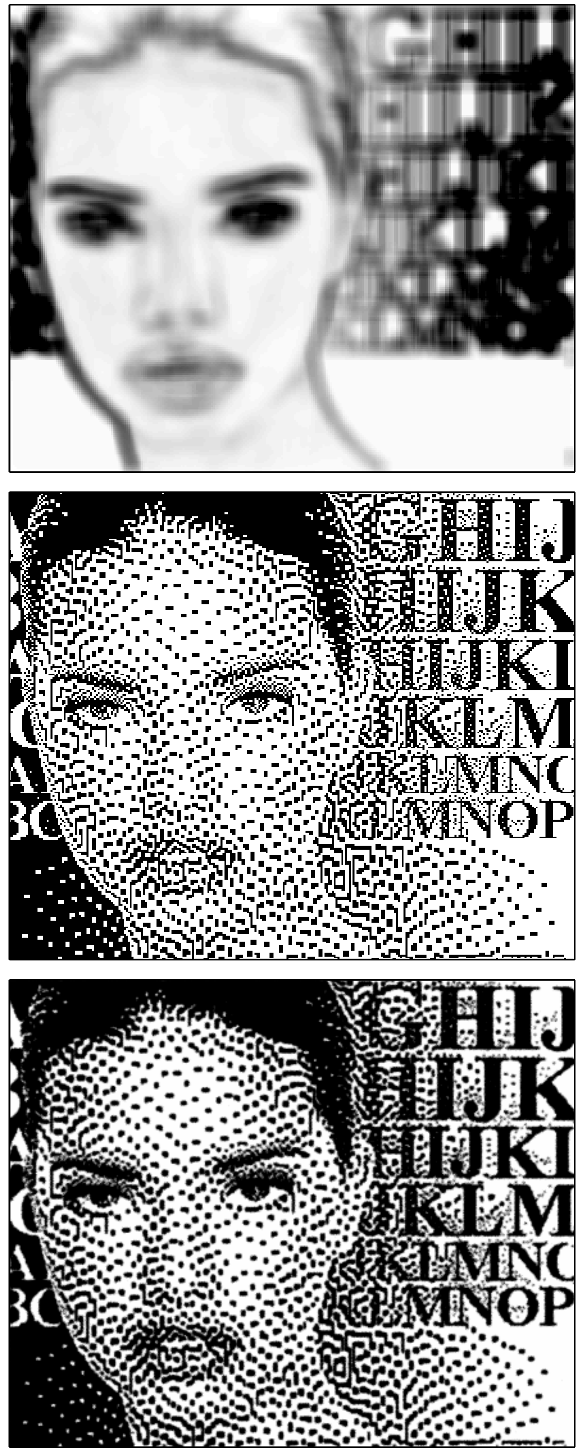

Figure 10: *The (top) frequency-dependent h used to generate the (middle) halftoned image and the (bottom) modeled output image.*